Report
R-24-08
September 2024

Recrystallisation kinetics of copper with phosphorus – experiments and modelling

Robert Sundström
Joacim Hagström
Henrik C.M. Andersson-Östling

SVENSK KÄRNBRÄNSLEHANTERING AB

SWEDISH NUCLEAR FUEL
AND WASTE MANAGEMENT CO

Box 3091, SE-169 03 Solna
Phone +46 8 459 84 00
skb.se

SVENSK KÄRNBRÄNSLEHANTERING

ISSN 1402-3091
SKB R-24-08
ID 2046856
September 2024

Recrystallisation kinetics of copper with phosphorus – experiments and modelling

Robert Sundström, Joacim Hagström, Henrik C M Andersson-Östling
Swerim AB

Summary

This study aims at quantifying and modelling recrystallisation behaviour for oxygen-free phosphorus doped copper (Cu-OFP). It is a continuation of a previous study done at Swerim in 2018 to 2020, Sundström et al. (2020). In the previous study, it was concluded that the recrystallisation temperature for annealing durations from 1 day to 6 months was between 175 and 250 °C since samples annealed at 175 °C had not recrystallised after 6 months while samples annealed at 250 °C showed recrystallisation from day 1 and had almost completely recrystallised within 1 week. The Cu-OFP in the present study was extracted from the same canister lid (TX219) that copper in the previous study had been extracted from. The experimental procedures were identical to those in Sundström et al. (2020) but the annealing temperatures and durations differed. As in the previous study, the material had been "pre-annealed" at 600 °C for 10 minutes and then cold rolled: this annealing step, excluding the cold rolling, is henceforth called *annealing at 600 °C* in this report. All material in this report underwent this annealing step.

After the annealing at 600 °C and subsequent cold rolling, the material was then annealed at twelve temperatures ranging from 195 to 259 °C and 16 durations ranging from eight hours to nine months. The recrystallisation response, measured as degree of recrystallisation (fraction of recrystallised material) in images taken in a scanning electron microscopy (SEM) using electron back scatter diffraction (EBSD) data, was used as input data in a model based on the Avrami equation. Only a subset of all the annealed samples were studied in the SEM, since it was known based on earlier analysis of other samples that they would not give useful input data to the model (i.e., recrystallisation was 0 or 100 %). Samples from three temperatures (241, 244, 247 °C) were also used for hardness measurements. The model used data from five temperatures from 241 to 255 °C and 13 durations from 0.47 to 60 days, a total of 20 different time–temperature combinations with the recrystallisation response as input data. An attempt at validation of the model was made by calculating the time duration for 50 % recrystallisation at three different temperatures (248, 254, 259 °C) and then annealing six samples, two for each time–temperature combination, at this predicted duration. The degree of recrystallisation in some of these samples were far below what was expected, and no conclusion could be made about the cause of this discrepancy. Nevertheless, the model was used to estimate time until recrystallisation for temperatures lower than those used as annealing temperatures. The model showed that at 175 °C, the duration until 50 % recrystallisation is on the order of 10^6 years. After 100 000 years at 175 °C, the recrystallised fraction would be 10^{-5} %.

Contents

1 Background

The recrystallisation behaviour of oxygen-free phosphorus doped copper (Cu-OFP) is of interest because of the extremely long timescales that are of relevance for a repository of spent nuclear fuel. SKB's repository method, KBS-3, uses canisters made from Cu-OFP, and in this study material from a canister lid was investigated. The lid is forged by pressing (up-setting) a cylinder from a continuously cast billet into to the final disc shape at around 700 °C (Hagström et al. 2022) and has a diameter of 1 050 mm (Jonsson et al. 2018). The maximum temperature of the copper in the repository is estimated to be 100 °C which it will reach within the first 10 years, after which it will slowly decrease to the temperature of the surrounding bedrock and remain there (SKB 2006). The degree of recrystallisation in copper is affected by temperature, cold deformation, and annealing time. Phosphorus enters solid solution in oxygen-free copper where it is known to increase the softening temperature (Smart and Smith 1946) and creep resistance of copper (MNC 1987) and to increase the recrystallisation temperature (Bowyer 1999). In contrast, cold deformation is known to decrease the softening temperature (MNC 1987). Phosphorus retards recovery and recrystallisation compared to pure copper (Hutchinson and Ray 1979). For example, 70 ppm phosphorus has been found to reduce growth rates of recrystallised grains in heavily cold worked copper by a factor of 2 000 compared to pure copper (Hutchinson and Ray 1979). Phosphorus also increases the activation energy for recrystallisation, for example from 80 to 151 kJ mol^{-1} for 99.998 % pure copper and phosphorus-doped copper with 1 600 and 7 600 ppm phosphorus additions, respectively (Hutchinson and Ray 1979).

The work presented in this report is aimed at quantifying the recrystallisation behaviour of Cu-OFP. In this study, which is a continuation of a previous study (Sundström et al. 2020) where recrystallisation and phosphorus distribution in Cu-OFP were studied, copper specimens have been annealed at different temperatures and times to measure the recrystallisation response. The degree of recrystallisation at different time–temperature combinations was then used as input data in a recrystallisation model based on the Avrami equation.

The goal of this study was to experimentally determine the recrystallisation behaviour of Cu-OFP at time spans less than a year, develop a model based on its behaviour and make predictions for whether the initial structure will persist over the very long timescales relevant for disposal of spent fuel. The results from the previous study (Sundström et al. 2020) showed that for durations up to 6 months, no recrystallisation occurred in cold deformed copper at 175 °C or below, which is well above the temperatures relevant in the repository. The threshold temperature for recrystallisation at durations up to 6 months, the temperatures at which recrystallisation starts to occur, was found to be between 175 and 250 °C. At 250 °C, samples showed recrystallisation from day 1 and had almost recrystallised completely within 1 week.

2 Method and experiments

2.1 Material, annealing and microscopy

The copper material tested in this project comes from a canister lid (TX219). The lid is forged by pressing (up-setting) a cylinder from a continuously cast billet into to the final disc shape at around 700 °C (Hagström et al. 2022) and has a diameter of 1 050 mm (Jonsson et al. 2018). The material used in the study was the same as that used in the previous study, and had been annealed before rolling (i.e., annealed at a higher temperature and shorter time duration than the subsequent annealing) at 600 °C for 10 minutes, quenched, and then cold rolled to a reduction of 50 %. Annealing at 600 °C was done to ensure that there was no effect on recrystallisation from potential variation in structure or properties in the lid, so that all specimens had a similar grain structure before cold rolling. The reduction provides a high degree of cold work in the specimens to provoke recrystallisation upon annealing. In the previous study, two reference samples were also manufactured: one that had only been annealed at 600 °C, and one that had been annealed before rolling at 600 °C and then cold rolled. This gave two well-defined states which roughly correspond to the two extremes of the annealing tests: one with recrystallised grains and no texture, and one with a heavily deformed non-recrystallised structure with a strong texture.

A short remark on terminology used in this report and Sundström et al. (2020). In Sundström et al. (2020), “ageing” was used to describe the process of holding the copper specimens at elevated temperatures for extended times. In this report, “annealing” has consistently been used to describe this process. The reasoning behind this change in terminology is that ageing is often used to describe a heat treatment consisting of holding a component at elevated temperatures for several hours or days. However, the goal of ageing is the precipitation of hardening phases, causing an increase in hardness and reduction in ductility. Annealing, by contrast, results in a decrease in hardness and increase in ductility, which is precisely what results when holding deformed Cu-OFP at elevated temperatures for long times.

In addition to this, “annealing at 600 °C” refers to the shorter annealing at 600 °C for 10 minutes, while “annealing” is reserved for the lower temperatures and longer durations (longer than 10 minutes, temperatures ranging from 75° to 450 °C in the previous study and 195° to 259 °C in the present study). All samples that were annealed to provoke recrystallisation had a prior anneal at 600 °C and were then rolled. Two reference samples were also made: one that was only annealed at 600 °C, and one that was annealed at 600 °C and then cold rolled. These were the reference specimens to which the hardness and microstructure of the samples annealed at lower temperatures can be compared to.

Square samples (ca 3 mm × 10 mm × 10 mm) of oxygen-free phosphorus doped copper (Cu-OFP) taken from the TX219 lid, and that had been milled (from 10 to 6 mm), were annealed at 600 °C for 10 minutes and cold rolled (50 % reduction, 6 to 3 mm). Then they were annealed at twelve different temperatures ranging from 195° to 259 °C (195, 210, 230, 237, 241, 244, 247, 248, 250, 254, 255, 259 °C) and 16 durations ranging from eight hours to nine months (0.33, 0.47, 1, 1.5, 2, 3, 4, 6.3, 7, 14, 21, 30, 42, 60, 90, 270 days). See also Table 3-3 for an overview of the samples.

One of these temperatures, 250 °C, had been used in the previous study on recrystallisation (Sundström et al. 2020), and the recrystallisation measurements for 250 °C from that study are also included in the present study. The present study includes additional durations for annealing at 250 °C, so the recrystallisation response for this temperature was a mix of old and new data.

Annealing was done in four different hot air furnaces (named B46A, B47A, B48A, B46B) at Swerim in Kista, Stockholm, and was performed by two different operators. The furnaces were of identical brand and dimensions. The fans in the furnaces did not work and could not be repaired. Convection can then cause temperature differences in the furnace. However, this was obviated by always placing the samples on a stand, consistently at the same height in each furnace, approximately in the middle of the furnace with respect to the height, width, and depth. Temperature control was achieved by using a thermocouple attached to a piece of copper placed next to the actual sample that was to be annealed, on the stand. The furnaces’ thermocouples are calibrated on a yearly basis. The temperatures given throughout the report are the nominal temperatures, and it is also the nominal temperatures that were

used in the modelling part of this work. The temperatures measured on the thermocouple were found to be within a maximum of 1 °C of the setpoint temperature for the furnace (the nominal temperature), usually within ± 0.5 °C or less.

After annealing, the samples were prepared for analysis in scanning electron microscopy (SEM) by grinding and polishing (grit 320 to 4 000, diamond polishing with 3 µm and 1 µm and electrolytic polishing), where the degree of recrystallisation was measured on surface areas ranging from 0.24 to 30 mm^2, with most of the analyses being done on surface areas of a few square millimetres in size. It was the sides of the samples (Figure 2-1) that were imaged and measured in electron microscopy.

Since the rolling direction of each sample was not known – this was not marked on the samples when they were cut from the rolled piece of copper – it is not known which direction was imaged in the microscopy or measured for hardness: the rolling direction and transverse direction (Figure 2-1) cannot be distinguished with certainty, although it can sometimes be assumed which direction has been imaged based on the observed grain morphology. In principle, the section used for these measurements does not affect the value of the fraction recrystallised obtained.

Electron backscatter diffraction (EBSD) was used to obtain recrystallisation fractions. The electron microscopy analyses were performed by one operator in one machine, Zeiss Gemini SEM 450 instrumented with EBSD detector Oxford Instruments Synergy and software package AZTEC. Recrystallised fractions were also evaluated using the built-in software package, which simply calculates the area fraction of the image which is recrystallised.

Samples from three temperatures (241, 244, 247 °C) had their grain sizes measured. Grain size was evaluated using the built-in software package in the SEM from the EBSD images, which calculates the equivalent circle diameter, i.e., a circle that has the same area as the grain. The sizes were calculated not taking twin boundaries into account. The grain sizes were small enough that a high number of grains (hundreds or thousands) could be captured in each image. The grain size distributions were often skewed, giving mean values that are not centred between the minimum and maximum values.

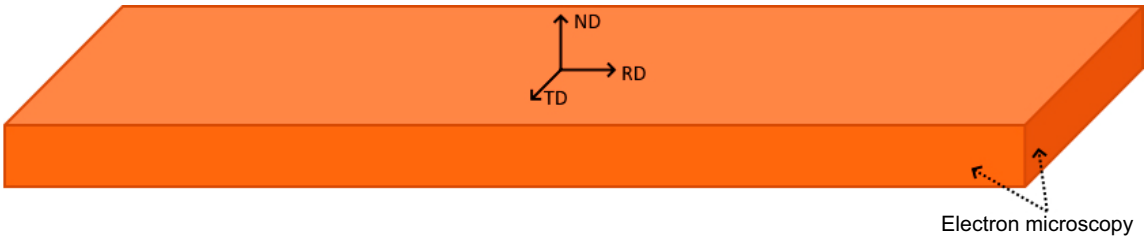

Figure 2-1. *Illustration of Cu-OFP sample showing the normal direction (ND, normal to upper surface plane), rolling direction (RD, parallel to upper surface plane), and transverse direction (TD, 90 degree from rolling direction, parallel to upper surface plane). Imaged sides are shown with dashed arrows (RD and TD). The illustration is not to scale, a real sample was square or rectangular in shape of approximate dimensions 3 × 10 × 10 mm (thickness × width × length). Note that the actual rolling direction was not known for the samples: it could be either in the direction of TD or RD.*

2.2 Model and hardness

An Avrami model for the recrystallisation was fitted to the data, with each data point consisting of the degree of recrystallisation for a time–temperature combination. The model was used to make predictions for time to achieve 50 % degree of recrystallisation for a few temperatures in a similar temperature range as that for the input data, to see if the model could be validated.

In the beginning of the project, a few initial annealing temperatures (195, 210 and 230 °C) and durations were used to find at which temperature recrystallisation proceeded from 0 to 100 % within nine months. One Cu-OFP sample for each time–temperature combination was annealed.

The recrystallisation results from these temperatures were reviewed and, based on these, three higher temperatures were chosen for another round of annealing, for durations ranging from 1 day to 60 days: 241, 244, 247 °C. Hardness (Vickers) measurements were also performed on these samples from the 241, 244 and 247 °C anneals. Hardness measurements were performed with a micro-indentation Vickers hardness tester, Q10A+, performed by one operator. Five indentations were made on each specimen using a 0.05 HV (50 g) indenter, on surfaces that had been prepared for electron microscopy as shown in Figure 2-1. Images for the hardness analysis were captured using a 100× magnification lens. The 0.05 HV indenter was used because it was used in the previous study, Sundström et al. (2020), and it has also been used by Li et al. (2023).

After the annealing at 241, 244 and 247 °C, a few more tests at shorter durations and higher temperature were used: 250 and 255 °C, from 8 hours to 3 days. Degree of recrystallisation data were obtained for these temperatures (241, 244, 247, 250, 255 °C) and collected into a data set that was fitted to a recrystallisation model using the Avrami equation. The model's predictive power was then tested by calculating the amount of time required for 50 % degree of recrystallisation at three different temperatures (248, 254, 259 °C), by annealing samples at these temperature–time combinations and measuring their degree of recrystallisation.

Some results were excluded throughout the project after reviews of results and discussions at Swerim and with SKB. At 195 °C, only one sample had the recrystallised fraction measured, the sample at 1 month's duration. This showed 0 % recrystallisation and no more samples from that temperature were studied. This was commonly done throughout the projects, to limit the number of samples that were studied metallographically. None of the samples from 210 °C had their recrystallised fractions measured.

Some previous analyses of the recrystallised fractions that had been performed by one operator were reviewed by another operator with more experience, for temperatures 244 and 247 °C and for durations 1, 7, 14, 30 and 60 days. These revised values were usually within 5 to 10 percentage points or expressed in relative terms within 20 % of the values previously measured by the other operator. It was also found that recrystallised fractions from 230 and 241 °C were contradictory to one another, so it was decided to remove all results from 230 and 241 °C and to anneal some additional samples at 241 °C to replace these data. For that reason, only the latest results from 241 °C are used as input to the modelling in this work. The excluded 241 °C samples were the samples that also had hardness measured. For that reason, the hardness data from 241 °C was also excluded. The hardness values, including the excluded values from 241 °C are shown struck through in Table 3-1. The excluded recrystallisation from data points from 230 and 241 °C are still shown in the results. Data points used in the model are shown in Table 3-2 and there, the excluded data is not shown. All the recrystallisation data from this project and the previous (Sundström et al. 2020) are shown in Table 3-3, including excluded data points.

In this report, EBSD and SEM images from a selection of temperatures are reported for the sake of brevity. However, recrystallised fractions from other temperatures and durations are reported in the results even though the images are not included.

2.3 Model equations

Deformation is a prerequisite for recrystallisation (Humphreys et al. 2017). Recrystallisation is affected by prior cold work (Rowe 1977, Humphreys et al. 2017) and is dependent on time and temperature and follows a behaviour where there is an initial incubation period, followed by recrystallisation that starts slowly and then reaches a maximum rate, and finally the rate of transformation becomes slower once the recrystallisation nears completion (Honeycombe 1968). The Avrami equation (Equation 2-1), also called Johnson–Mehl–Avrami–Kolmogorov (JMAK) equation, can be used to describe recrystallisation kinetics (Humphreys et al. 2017, Honeycombe 1968), where X_s is the recrystallised fraction (range of values from 0 to 1) for a given time duration t, $t_{0.5}$ is the time duration to achieve a recrystallised fraction of 0.5 (50 %) (Honeycombe 1968) and n is an empirical exponent that is obtained by fitting to measurements. A typical recrystallisation behaviour described with this equation for two different temperatures in a linear–logarithmic diagram is shown in Figure 2-2: the rate of recrystallisation is slow at first, then becomes exponential and eventually tapers off.

$$X_s = 1 - \exp\left[\ln(1/2)\left(\frac{t}{t_{0.5}}\right)^n\right] \qquad \text{Equation 2-1}$$

The time until 50 % recrystallised fraction ($t_{0.5}$), is known to follow Equation 2-2 (Honeycombe 1968) for a given temperature (T). Equation 2-2 also contains the universal gas constant (R) and fitting parameters (Q, A) which are determined from experimental data, where Q corresponds to the activation energy ([J mol^{-1}]). All the parameters are listed in Table 2-1.

Together, Equation 2-1 and Equation 2-2 describe a model for recrystallisation which can be used to predict recrystallised fractions after a certain time (Equation 2-1) and the time until 50 % recrystallised fraction is achieved (Equation 2-2).

$$t_{0.5} = Aexp\left(\frac{Q}{RT}\right) \qquad \text{Equation 2-2}$$

Equation 2-1 was rewritten as Equation 2-3, and linear regression was used to obtain the slope (B_0) and intercept (B_1) in Equation 2-4 using the recrystallisation response (X) for each time duration (t) at a temperature, i.e., by plotting $ln(-ln(1-X))$ against $ln(t)$ and fitting a linear trendline to this data, giving a line for each temperature with the values for slope (B_0) and intercept (B_1). The model used data from five temperatures (241, 244, 247, 250, 255 °C) and 13 durations (0.47, 0.33, 1, 1.5, 2, 3, 6.3, 7, 14, 21, 30, 42 and 60 days), a total of 20 different time–temperature combinations with the recrystallisation response as input data. Each temperature then has a specific value of the slope (B_0), and here it was decided to take an average value of all values of n rather than using separate values for each temperature when proceeding with the modelling. The colour coding and underlining (solid or dashed) shows which part of the equations that correspond to each other. n corresponds to B_0 (slope) and since B_1 (intercept) contains $t_{0.5}$ (Equation 2-5) it was rewritten as Equation 2-6, and $t_{0.5}$ in Equation 2-2 was rewritten as Equation 2-7. Equation 2-6 is used to calculate $\ln(t_{0.5})$ since B_1 and n are known, and then the values for $\ln(t_{0.5})$ are plotted against the inverse of temperature (1/T). A linear regression was made to this data, and the constants C_0 (slope) and C_1 (intercept) are then found. Equation 2-8 shows which part of Equation 2-7 it corresponds to by colour coding and underlining. From C_0 (slope) and C_1 (intercept), values for A and Q are found. Having found values for A, Q, and n, diagrams such as that shown in Figure 2-2 can be plotted for each temperature. Each temperature then has a set of data points (recrystallisation response for a time duration) with a curve fit, described by Equation 2-1. Equation 2-2 can then be used to calculate the time until 50 % recrystallisation for any temperature and Equation 2-1 can be used to calculate the recrystallised fraction for a given time. Equation 2-2 was used to predict the time until 50 % recrystallisation for three temperatures (248, 254, 259 °C), and then 2 samples at each temperature was annealed for the predicted time duration. This was done to validate the model, to see if it had any predictive power.

The samples at each temperature were annealed for the predicted time duration. The sample at 254 °C had been annealed at 237 °C for 85 days before the temperature was increased to 254 °C, since it became known, based on results from 248 and 259 °C, that no recrystallisation had likely taken place at 237 °C for that duration. Initial guesses of the fitting parameters in Table 2-1 were obtained using mathematical operations (exponential, logarithm) and linear regression (linear trend line) in Excel. These initial guesses were then used in Python to obtain an optimized fit. The Python code used scipy.optimize.curve_fit, which employs non-linear least squares to fit a function to data, using the Levenberg-Marquardt algorithm (Levenberg 1944) through least squares (minimizing sum of squares of a set of equations). The values for the initial guess and for the optimized fit are shown in Table 3-5.

$$\ln(-\ln(1-X)) = n\ln(t) + \ln(0.693) - n\ln(t_{0.5}) \quad \text{Equation 2-3}$$

$$y = B_0 x + B_1 \quad \text{Equation 2-4}$$

$$B_1 = \ln(0.693) - n\ln(t_{0.5}) \quad \text{Equation 2-5}$$

$$ln(t_{0.5}) = \frac{B_1 - \ln(0.693)}{n} \quad \text{Equation 2-6}$$

$$ln(t_{0.5}) = \left(\frac{Q}{R}\right)\frac{1}{T} + \ln(A) \quad \text{Equation 2-7}$$

$$y = C_0 x + C_1 \quad \text{Equation 2-8}$$

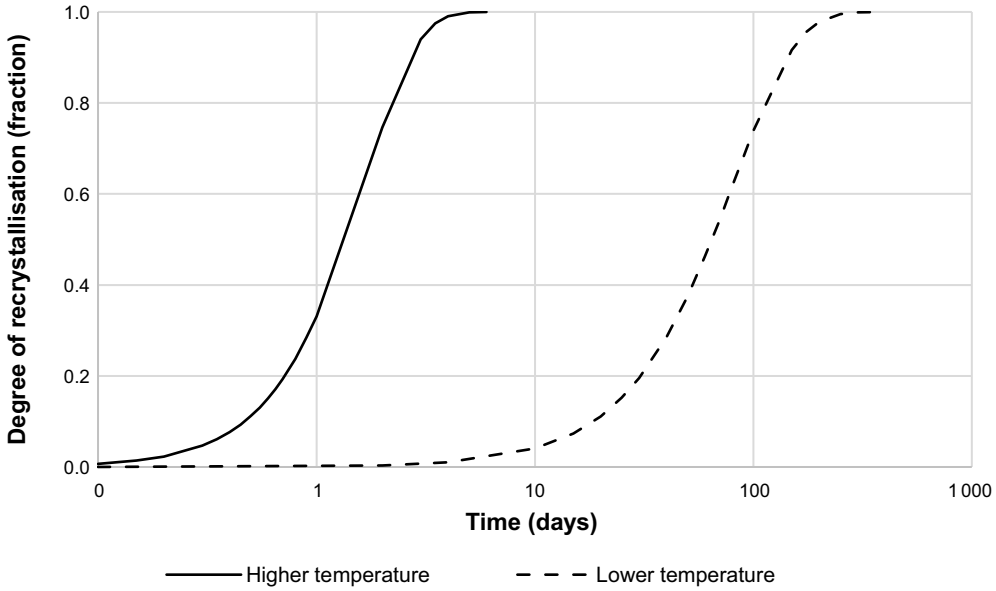

Figure 2-2. *Typical recrystallisation behaviour for two different temperatures in a linear–logarithmic diagram.*

Table 2-1. Parameters in equations used to describe a model for recrystallisation.

Parameter	Description
t	time (days)
X_s	recrystallised fraction
$t_{0.5}$	the time taken to achieve a 50 % recrystallised fraction (days)
A	constant (fitting parameter) (days)
n	constant (fitting parameter)
Q	activation energy (fitting parameter) (J mol^{-1})
R	gas constant (8.314 J $mol^{-1}K^{-1}$)
T	absolute temperature (K)

3 Results

3.1 Hardness

The hardness has been measured in a factorial experiment involving annealing temperature and holding time. Table 3-1 shows the difference between the hardness of Cu-OFP specimens annealed at 600 °C, the hardness after annealing at 600 °C and a subsequent cold deformation by rolling, as well as the hardness of the annealed Cu-OFP for temperatures 241, 244 and 247 °C.

However, the values from 241 °C are struck through because these samples were excluded from the recrystallised fractions data. Hardness of two samples that were only annealed at 600 °C and annealed at 600 °C and then rolled is also included in Table 3-1, which were reported in Sundström et al. (2020).

Table 3-1 also shows the average values of each duration and temperatures, to illustrate how the hardness changes. The table has been coloured in shades of grey according to the similarity of the average values; columns with average values exceeding HV 90, which is closer to that of the rolled specimen, are shown in dark grey, while columns with average values below that, which is closer to that of the specimen annealed at 600 °C, are shown in light grey.

Table 3-1. Hardness (HV 0.05) of samples annealed at 241 °C, 244 °C, and 247 °C.

	Annealed at 600 °C and cold rolled	**Annealed at 600 °C**				
	131.0	45.1				
	115.0	49.9				
	117.0	43.5				
	130.0	44.1				
	125.0	46.4				
Average	123.6	46				
Annealed at 600 °C, cold rolled and then annealed at temperature:	**1 day**	**4 days**	**1 week**	**2 weeks**	**1 month**	**2 months**
	~~125.0~~	~~115.0~~	~~120.0~~	~~116.0~~	~~128.0~~	~~132.0~~
~~**241 °C**~~	~~113.0~~	~~121.0~~	~~125.0~~	~~125.0~~	~~120.0~~	~~125.0~~
	~~118.0~~	~~120.0~~	~~135.0~~	~~133.0~~	~~125.0~~	~~124.0~~
	~~124.0~~	~~127.0~~	~~123.0~~	~~113.0~~	~~109.0~~	~~122.0~~
	~~113.0~~	~~115.0~~	~~112.0~~	~~119.0~~	~~127.0~~	~~113.0~~
~~***Average***~~	~~*118.6*~~	~~*119.6*~~	~~*123.0*~~	~~*121.2*~~	~~*121.8*~~	~~*123.2*~~
	120.0	118.0	91.8	78.6	60.0	65.2
	117.0	106.0	86.3	72.8	55.6	68.1
244 °C	114.0	115.0	61.5	96.0	75.6	70.5
	120.0	81.9	86.8	58.4	59.9	64.1
	120.0	114.0	94.9	66.5	83.8	78.0
Average	*118.2*	*107.0*	*84.3*	*74.5*	*67.0*	*69.2*
	115.0	62.3	104.0	58.7	58.1	58.2
	116.0	111.0	109.0	74.3	55.2	59.1
247 °C	128.0	73.9	125.0	56.2	55.8	61.4
	114.0	116.0	75.4	55.7	52.3	58.6
	115.0	120.0	99.7	63.5	54.9	55.9
Average	*117.6*	*96.6*	*102.6*	*61.7*	*55.3*	*58.6*

Hardness decreases as recrystallisation proceeds (Davis 2001) which is clearly captured in these measurements. One can see how the hardness measurements decrease with the first factor temperature and that the hardness also decreases with the second factor holding time at 244 and 247 °C. This is apparent despite the large scatter, possibly caused by the method used (micro-hardness), the mix of non-recrystallised and recrystallised grains being sampled and the lack of knowledge about which section was measured, the transverse or the rolling direction (Figure 2-1); see discussion in Section 4.2. The scatter is lowest for the shortest and longest durations (1 and 60 days) and for samples that were annealed at 600 °C and cold rolled or only annealed at 600 °C. These samples have either little or near complete recrystallisation: compare pair-wise the figures Figure 3-3 and Figure 3-4, Figure 3-8 and Figure 3-9, Figure 3-10 and Figure 3-11, where the grain structure is shown for these samples.

Figure 3-1 shows the measured hardness values for annealing temperatures 244, 247 °C and values for specimens annealed at 600 °C and those annealed at 600 °C then cold rolled. The averages for each temperature and duration are plotted as filled symbols while the individual measurements are plotted as hollow symbols. The hardness values for Cu-OFP annealed at 600 °C and the rolled Cu-OFP are shown as black or grey dashes and plotted at the left extreme of the diagram for a time of 10 minutes (0.167 hours) since this was the annealing time at 600 °C. The averages are not shown for this data.

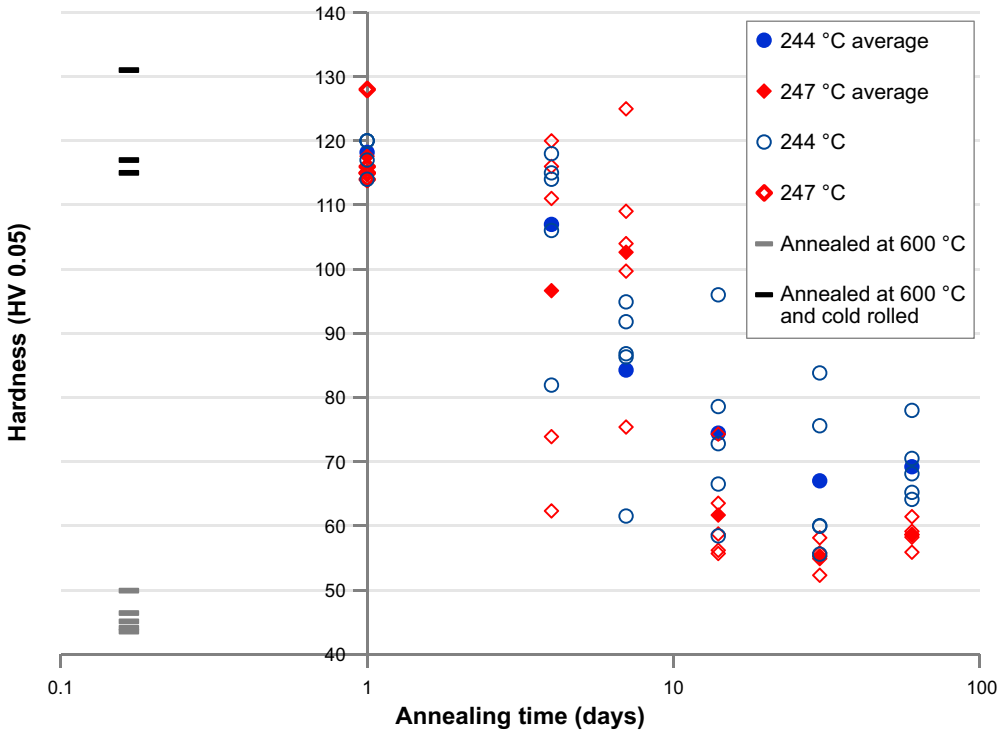

Figure 3-1. *Hardness (Vickers, HV 0.05) measurements of 244 and 247 °C for annealing durations ranging from 1 day to 60 days. Including data for specimens annealed at 600 °C before rolling, and annealed at 600 °C then cold rolled, from Sundström et al. (2020).*

3.2 Grain structures

Using data obtained by EBSD, SEM images can be coloured according to an Inverse Pole Figure (IPF) colour key (Figure 3-2). Such images of the Cu-OFP annealed at 600 °C and the Cu-OFP annealed at 600 °C with subsequent cold rolling, are shown in Figure 3-3 (cold rolled) and Figure 3-4 (annealed at 600 °C). The annealed specimens are shown in Figure 3-5 to Figure 3-11. A select number of durations from four temperatures are shown: 241, 244, 247, 255 °C. These were chosen because they had the highest number of time–temperature combinations to choose from, making it possible to show how the recrystallisation proceeds with time. Some previous results from 250 °C for 1 day to 12 months can also be seen in an earlier publication, Sundström et al. (2020). Different colours thus indicate different crystal orientations, and grain boundaries are shown in black based on a specified misorientation criterion of 15 degrees. Low angle boundaries are shown based on a criterion of either 1 or 0.5 degrees. Respectively, the annealed and cold rolled specimens represent the two extremes which have been captured in the recrystallisation studies: the non-recrystallised, highly deformed rolled condition (Figure 3-3) and the fully recrystallised annealed condition free from a deformed substructure (Figure 3-4). These specimens and images are from the previous investigation, Sundström et al. (2020). These extremes are also reflected in the hardness measurements (Figure 3-1) where the fully recrystallised condition has a hardness much lower than that of the non-recrystallised rolled condition.

At 241 °C, a recrystallised fraction of 2 % is seen after 7 days (Figure 3-5), which develops to 18 % recrystallised fraction after 21 days (Figure 3-6) and 24 % after 42 days (Figure 3-7). At 244 °C, recrystallisation is observed from 1 day of annealing, which is seen in Figure 3-8 where an Inverse Polar Figure mapping (IPF) has been overlaid with grain boundaries. When this is done, a non-recrystallised specimen which is heavily deformed due to the rolling, shows a deformed substructure which is visible as a grid of black lines overlaid on the image. When the specimen is partially recrystallised, recrystallised grains in this substructure show up as brightly coloured areas. Another way of showing recrystallised fractions, without showing the crystal orientations, is by using green-grey and red colours for non-recrystallised and recrystallised areas respectively, which is done for Figure 3-5 to Figure 3-7 and Figure 3-12 to Figure 3-15. Only the durations of 1 day and 2 months are shown 244 °C and for 247 °C, for the sake of brevity. At 244 °C the sample is fully recrystallised after 2 months (Figure 3-9). The same is true for 247 °C, seen after 1 day in (Figure 3-10) and 2 months in (Figure 3-11). At 255 °C, the recrystallisation proceeds fast, from 5 % after 8 hours (Figure 3-12), to 42 % after 1 day (Figure 3-13). A much larger area was analysed for the sample at 1 day (Figure 3-14), and there was a difference in recrystallised fraction of 1.16 percentage points, with the larger area having a lower percentage. After 2 days, the recrystallised fraction was 68 % (Figure 3-15). A similar comparison was done for a sample at 254 °C after 1.5 days of annealing, although not shown with images here, where it was found that a smaller area had a fraction of 81 % and a larger area had a fraction of 75 %, a difference of 6 percentage points. In all cases where such comparisons were made, the value from the larger area was used.

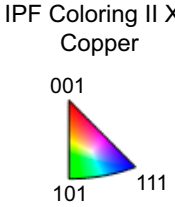

Figure 3-2. *Colour key for orientations in Inverse Polar Figures.*

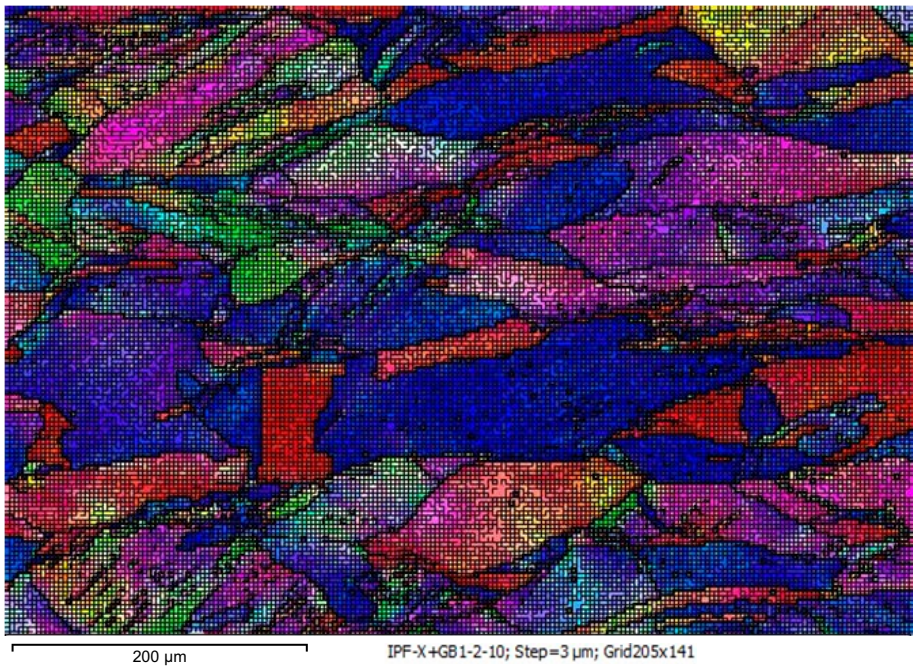

Figure 3-3. *Specimen annealed at 600 °C then cold rolled. A heavily deformed and non-recrystallised grain structure is seen. Scale bar is 200 µm.*

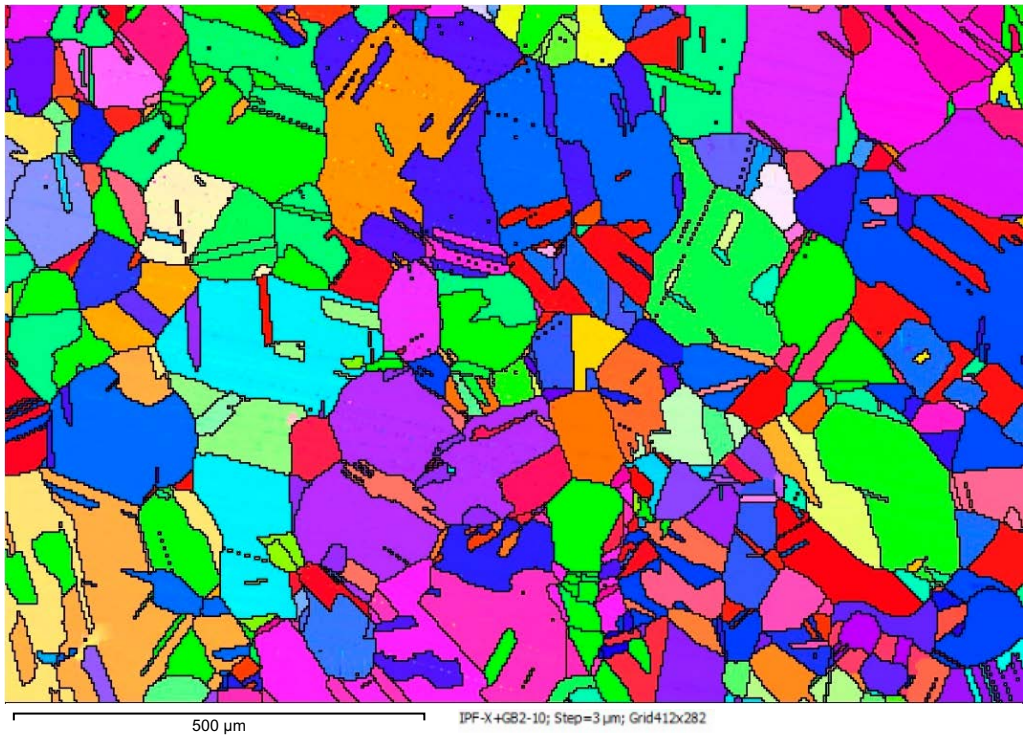

Figure 3-4. *Annealed at 600 °C. A fully recrystallised grain structure is seen. Scale bar is 500 µm.*

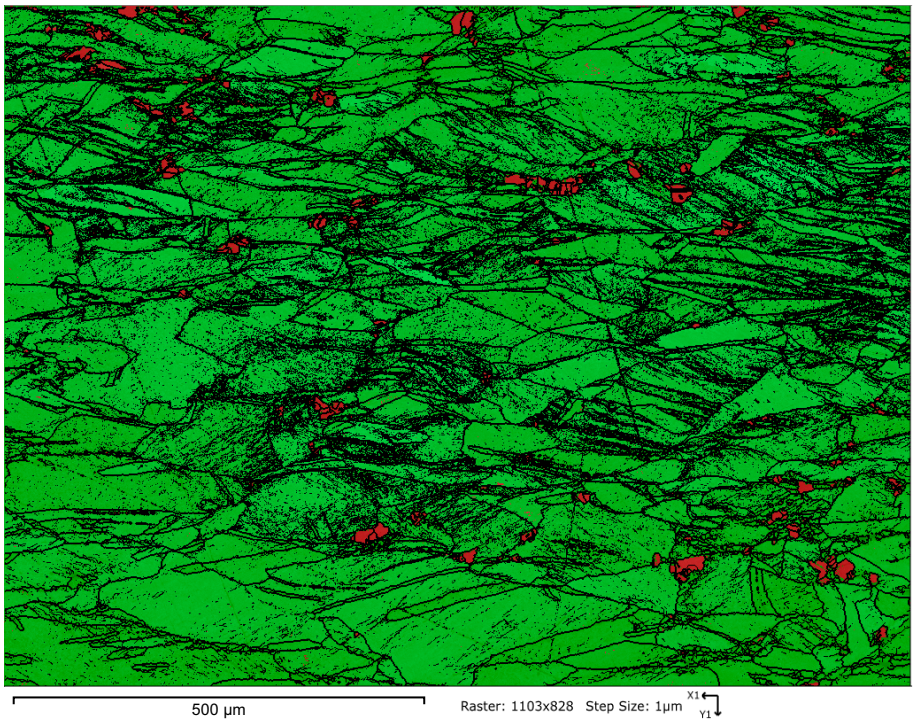

Figure 3-5. *241 °C, 7 days. A heavily deformed grain structure with some recrystallisation is seen. Scale bar is 500 µm.*

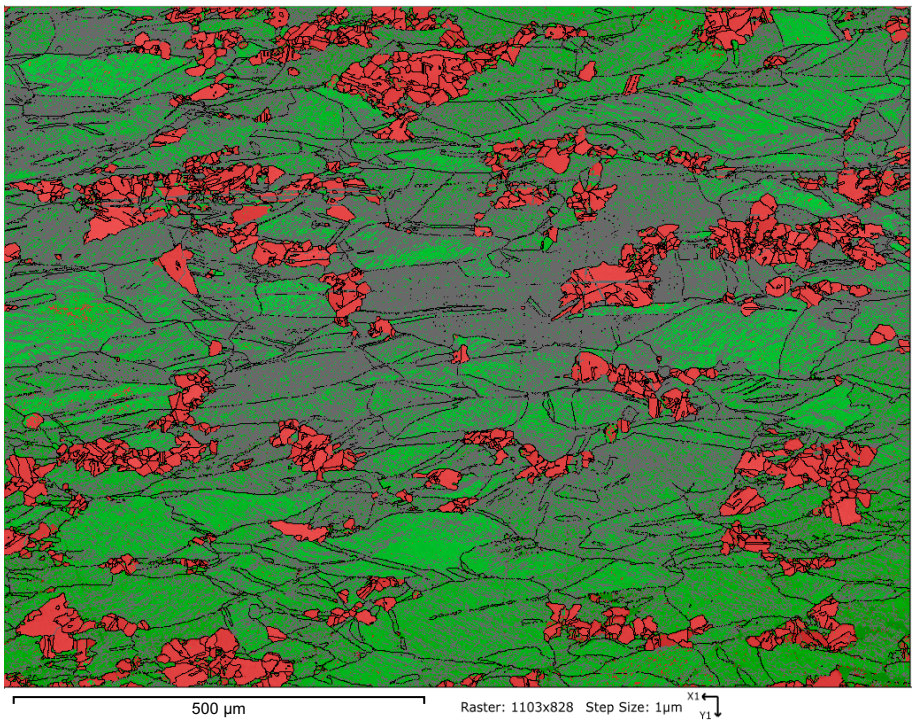

Figure 3-6. *241 °C, 3 weeks. A heavily deformed grain structure with developed recrystallisation. Scale bar is 500 µm.*

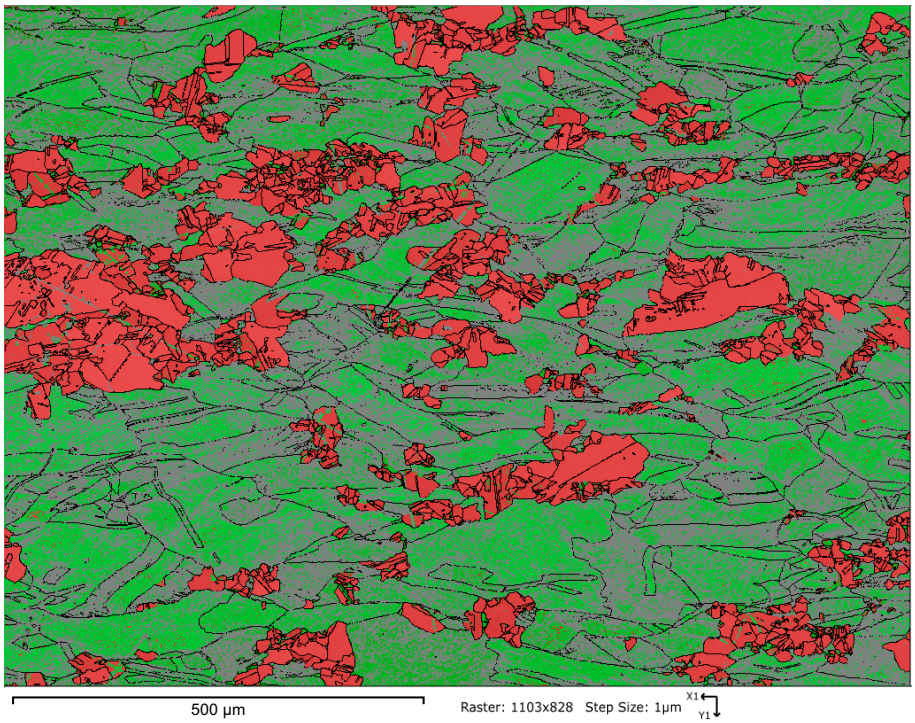

Figure 3-7. *241 °C, 6 weeks. A heavily deformed grain structure with developed recrystallisation. Scale bar is 500 µm.*

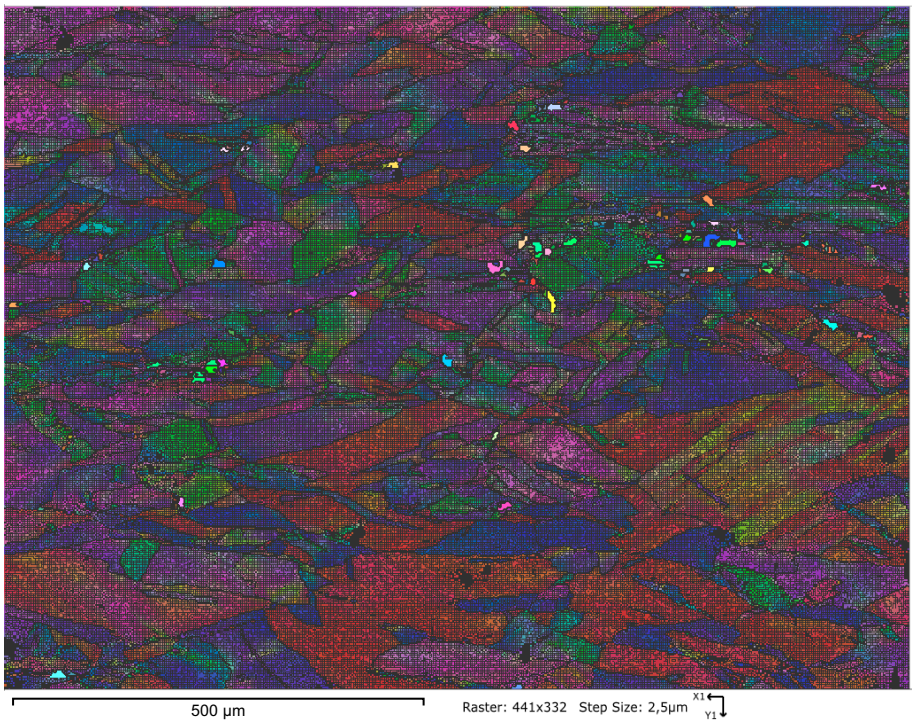

Figure 3-8. *244 °C, 1 day. A heavily deformed grain structure with recrystallisation just having started, seen as brightly coloured areas in the darker matrix. Scale bar is 500 µm.*

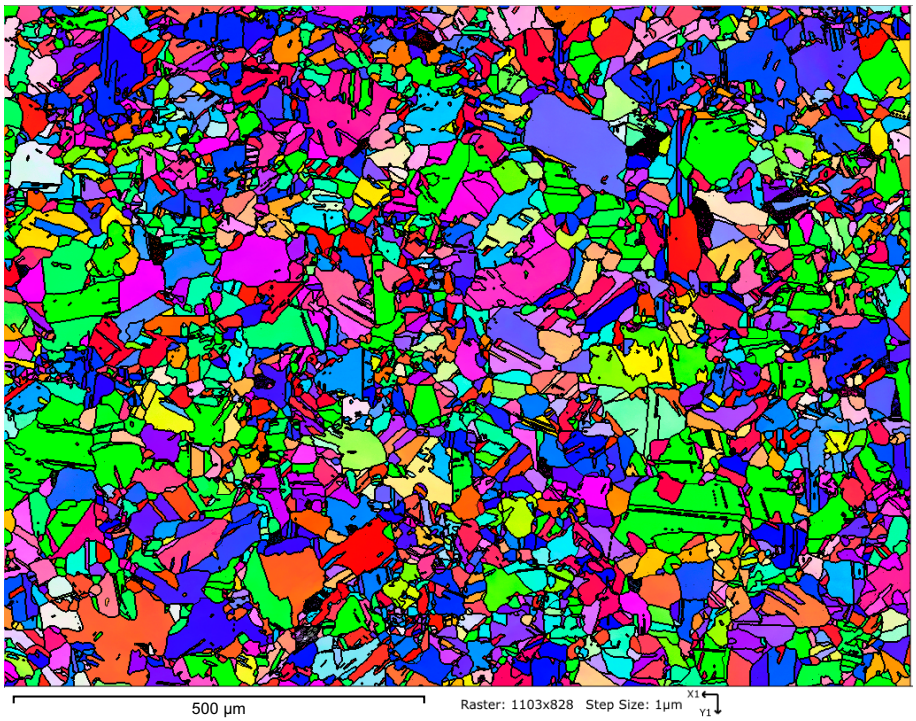

Figure 3-9. *244 °C, 2 months. A grain structure that is almost completely recrystallised. Scale bar is 500 µm.*

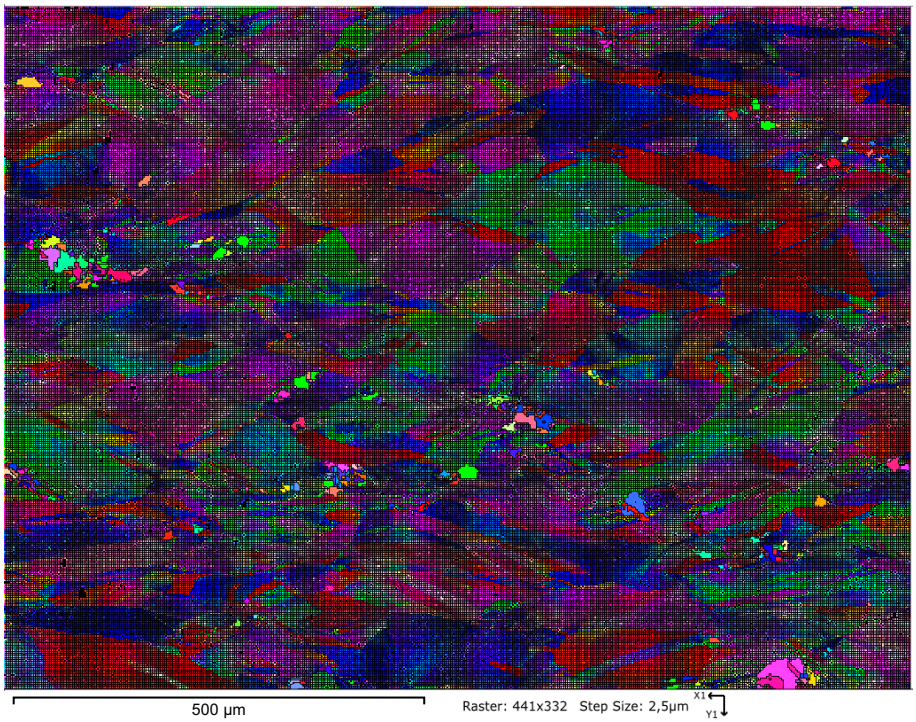

Figure 3-10. *247 °C, 1 day. A heavily deformed grain structure with recrystallisation just having started, seen as brightly coloured areas in the darker matrix. Scale bar is 500 µm.*

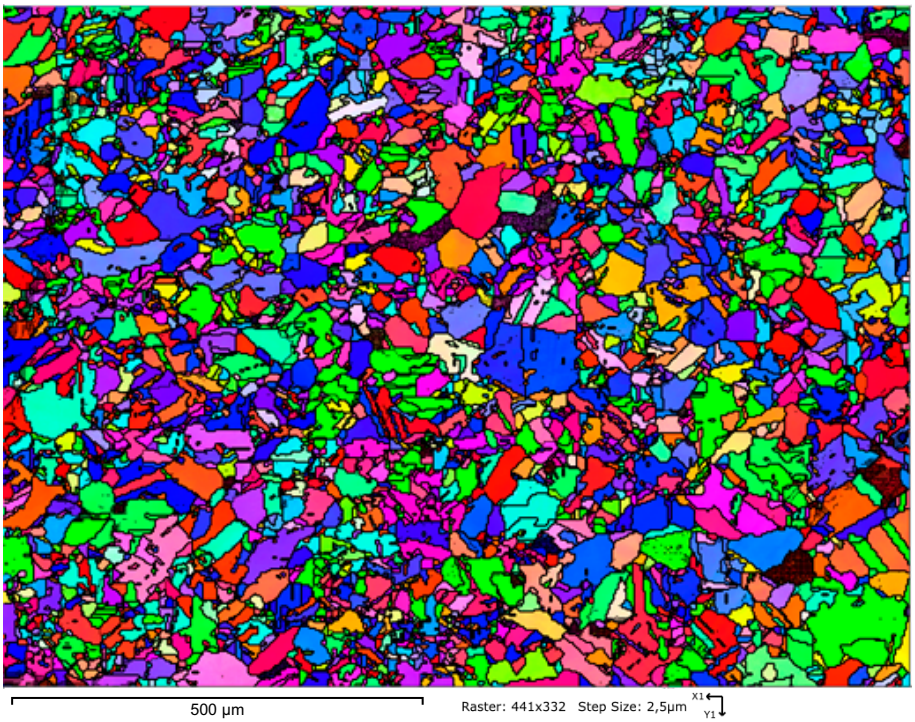

Figure 3-11. *247 °C, 2 months. A grain structure that is almost completely recrystallised. Scale bar is 500 µm.*

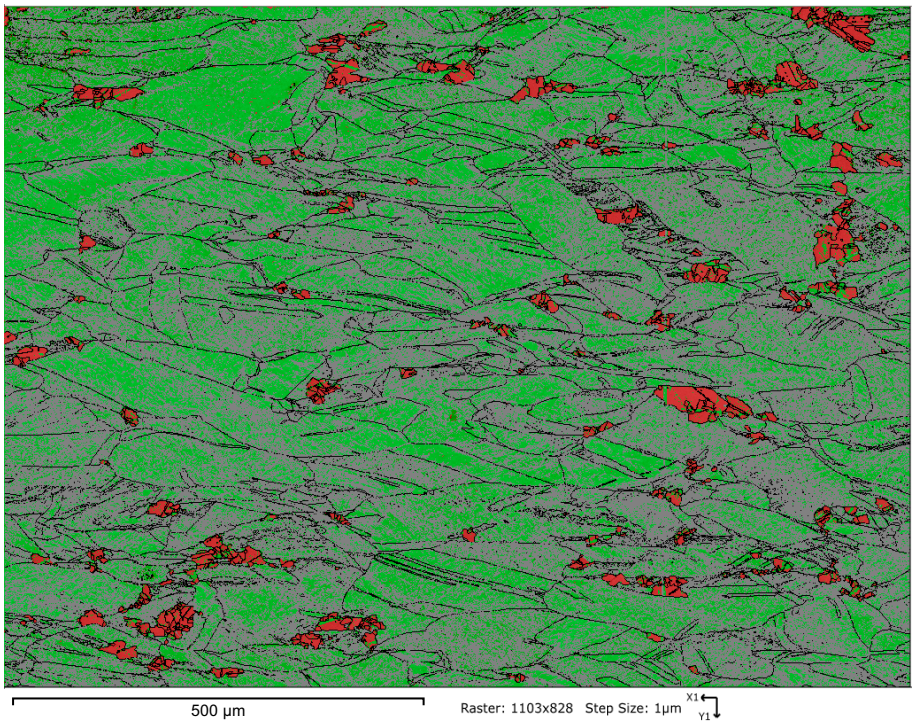

Figure 3-12. *255 °C, 8 hours. Scale bar is 500 µm.*

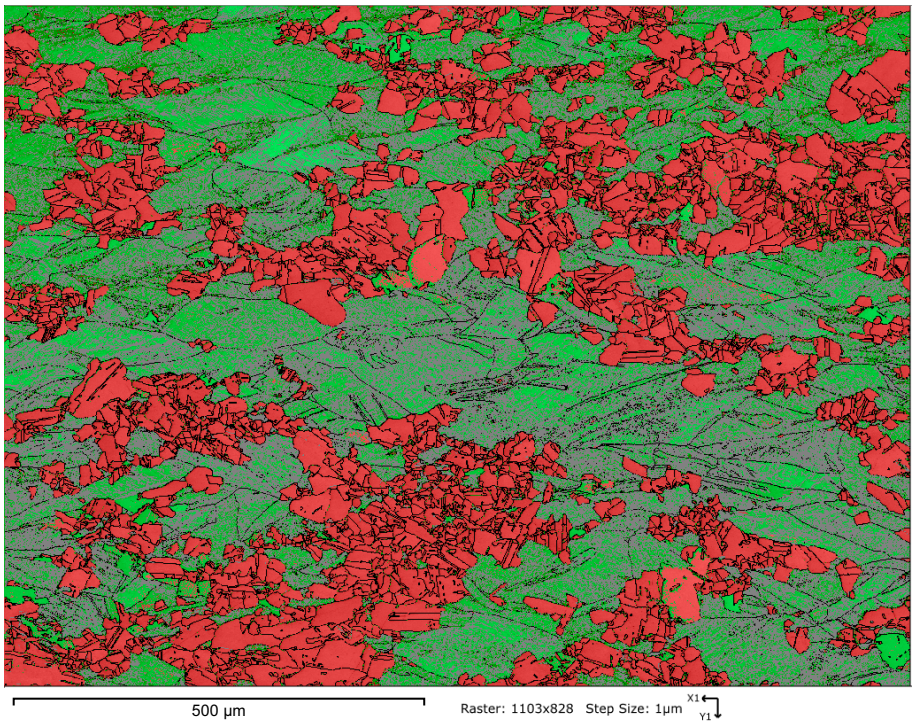

Figure 3-13. *255 °C, 24 hours. Scale bar is 500 µm.*

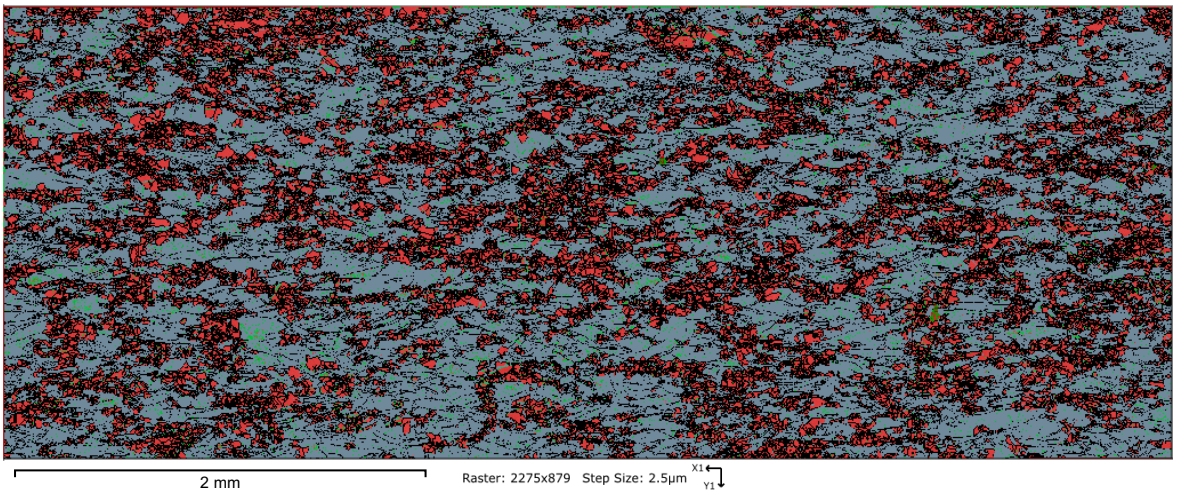

Figure 3-14. *255 °C, 24 hours. A larger area than in Figure 3-13 is shown. Scale bar is 2 mm.*

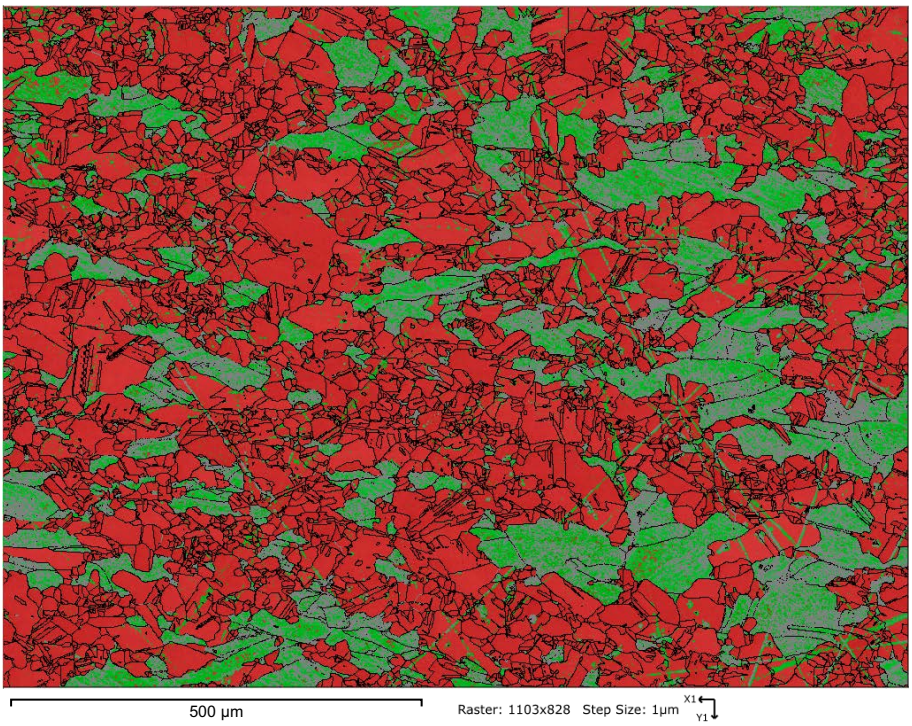

Figure 3-15. *255 °C, 48 hours. Scale bar is 500 µm.*

3.3 Recrystallised fractions and grain size

The recrystallised fractions, 26 fractions from 26 samples, are shown in Table 3-2. Values that were used for validation of the model, six in total, are shown with grey shaded background. These three time–temperature combinations had two samples each. The rest, with a white background (20 fractions), was used as input data for the model. These combinations are also shown as a diagram in Figure 3-16.Values with asterisk (*) in Table 3-2 are from the previous project (Sundström et al. 2020). The recrystallised fractions are shown in Figure 3-17.

Note that the sample that was annealed at 254 °C had been annealed at 237 °C for 85 days, and then the temperature was increased to 254 °C while still inside the furnace and it was kept there for the duration stated in Table 3-2 (1.5 days). This was done because four other samples at 248 and 259 °C had recrystallised to a much lesser degree than was anticipated, so it was reasonable to assume that the sample at 237 °C had not recrystallised.

Table 3-2. Recrystallised fractions (%). Cells with grey shaded background contain values that were used for validation of the model. Value with asterisk (*) are from the previous project, Sundström et al. (2020).

Temperature (°C)	Time (days)												
	0.33	0.47	1	1.5	2	3	6.3	7	14	21	30	42	60
241								2		18		24	
244			0.6			2		42	80		95		98
247			2.5					45	80				98
248							0.1, 0.5						
250			10*		15	26		90*					
255	5		42		68								
254				65, 75									
259		6, 8											

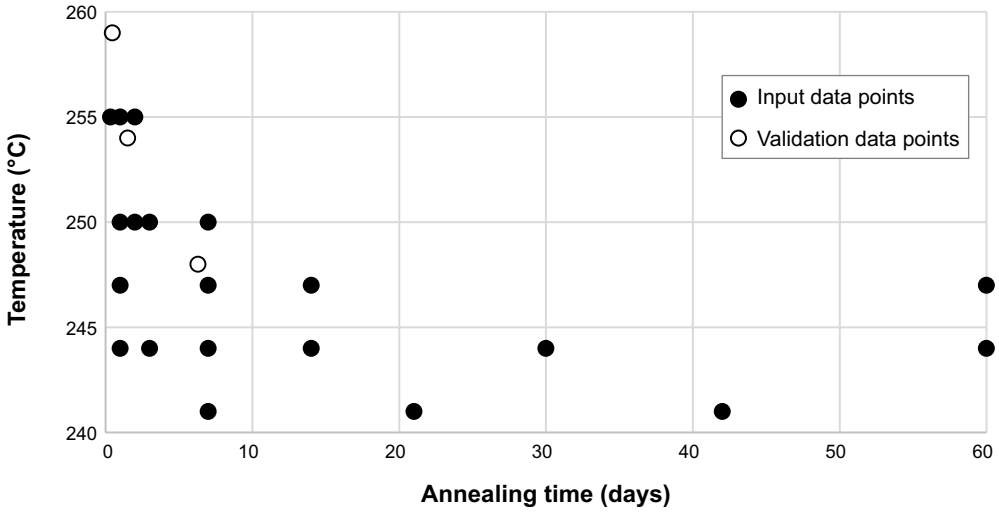

Figure 3-16. *Time-temperature combinations from Table 3-2 showing the distribution of specimens over time and temperature range.*

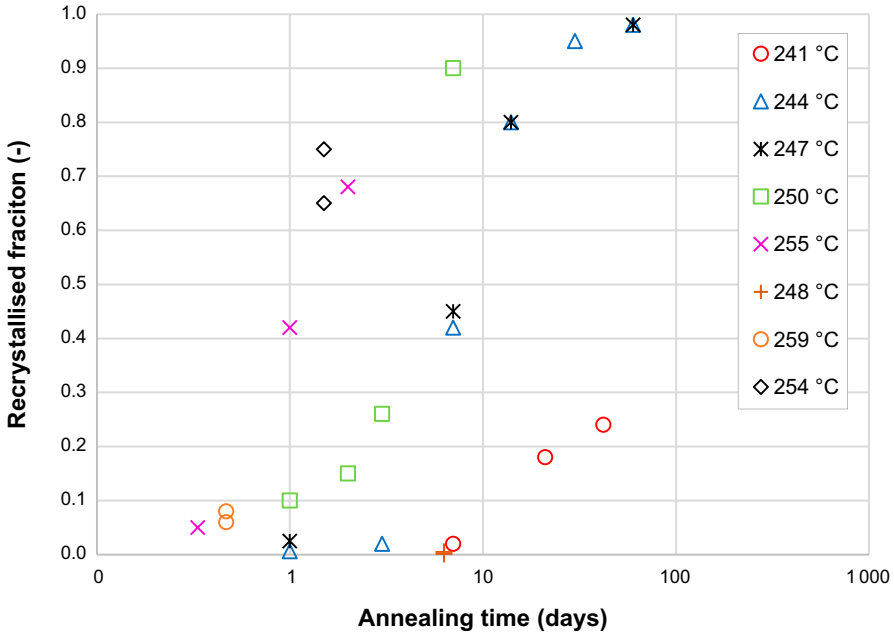

Figure 3-17. *Recrystallised fractions obtained from EBSD images for samples in Table 3-2.*

In addition to showing the recrystallisation data used for the model, the data from Sundström et al. (2020) are shown together with the data from the present project in Table 3-3, to give an overview of the recrystallised fractions obtained for different time–temperature combinations in the range 75 °C to 450 °C and a few hours to 12 months. Values that were not useful to the model (0 or 100 %) are also shown in that table, as are the excluded values, which have been struck through.

Grain sizes for annealing temperatures 244 °C and 247 °C are shown in Table 3-4 and plotted in Figure 3-18. Note that these samples where grain size was measured were not fully recrystallised. Note also that some grain size distributions were skewed, so the mean is not centred between the minimum and maximum values.

Table 3-3. Table of recrystallised fractions for each temperature and duration studied in the present study and Sundström et al. (2020). Struck through values are the removed data points.

Temperature (°C)	Time (days) 0.33	0.47	1	1.5	2	3	4	6.3	7	14	21	30	42	60	90	180	270	360
75	-	-	0	-	-	-	-	-	0	0	-	0	-	0	0	0	-	-
125	-	-	0	-	-	-	-	-	0	0	-	0	-	0	0	0	-	-
175	-	-	0	-	-	-	-	-	0	0	-	0	-	0	0	0	-	-
195	-	-	-	-	-	-	-	-	-	-	-	0	-	-	-	-	-	-
210	-	-	-	-	-	-	-	-	-	-	-	-	-	-	-	-	-	-
230	-	-	~~0~~	-	-	-	-	-	~~0~~	~~4~~	-	-	-	~~54~~	-	-	-	-
237	-	-	-	-	-	-	-	-	-	-	-	-	-	-	-	-	-	-
241	-	-	~~0~~	-	-	-	-	-	~~0~~, 2	~~0~~	18	~~0~~	24	~~0~~	-	-	-	-
244	-	-	0.6	-	-	2	-	-	42	80	-	95	-	98	-	-	-	-
247	-	-	2.5	-	-	-	-	-	45	80	-	-	-	98	-	-	-	-
248	-	-	-	-	-	-	-	0.1, 0.5	-	-	-	-	-	-	-	-	-	-
250	-	-	10	-	15	26		-	90	-	-	-	-	-	100	100	-	100
254				65, 75	-	-	-	-	-	-	-	-	-	-	-	-	-	-
255	5	-	42	-	68	-	-	-	-	-	-	-	-	-	-	-	-	-
259		6, 8	-	-	-	-	-	-	-	-	-	-	-	-	-	-	-	-
350	-	-	100	-	-	-	-	-	100	100	-	-	-	-	-	-	-	-
450	-	-	100	-	-	-	-	-	100	100	-	-		-	-	-	-	-

Table 3-4. Equivalent Circle Diameter (ECD) grain sizes for durations and temperatures which were sufficiently recrystallised to measure the grain size.

Temperature (°C)	Duration day(s)	Mean (µm)	Max (µm)	Min (µm)	N (-)	Standard error (-)
244	**7**	24	76	9	630	0.57
244	**14**	30	183	9	1 054	0.66
244	**30**	26	108	9	1 131	0.50
244	**60**	27	159	4	906	0.79
247	**7**	24	117	9	987	0.50
247	**14**	27	126	9	1 150	0.60
247	**60**	28	124	9	958	0.62

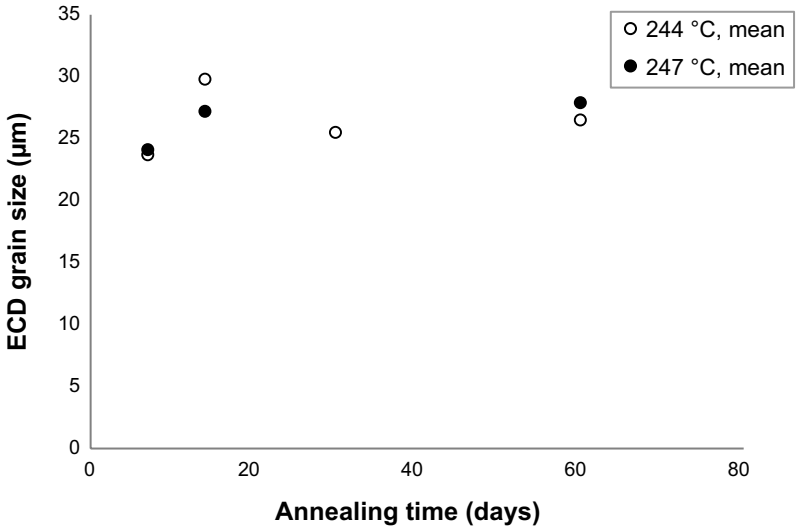

Figure 3-18. *Equivalent circle diameter (ECD) mean grain sizes for samples annealed at 244 °C and 247 °C.*

3.4 Modelling

Based on the fractions in Table 3-2, excluding the validation data points, a model could be fitted to 20 data points. This has been well described in Chapter 2. The model's parameters are listed in Table 3-5. Note that the R^2 and RMSE values in Table 3-5 are based on the curve fitting to the 20 data points from Table 3-2, so these values do not capture how well the model's curve fits to the validation data points. The value of the initial guess of n (slope, see Chapter 2 for description) was based on an average of five values which is shown in Table 3-6. The initial guesses were then used to obtain fitted values in Python based on an optimization algorithm described in Chapter 2. The curve fits are shown in Figure 3-19.

Time until 50 % recrystallisation for four temperatures were calculated (Table 3-7) using the fitting parameter values obtained from Python. The samples were annealed at these time durations to see if the model could be validated, the strength of its predictive power. Initially, only three temperatures were in the test matrix (237, 248, 259 °C) but after the recrystallised fractions for 248 and 259 °C had been determined and were shown to be lower than predicted (Table 3-7), it was decided to change the temperature for the samples being annealed at 237 °C to a higher temperature, 254 °C. This was done after 85 days of annealing at 237 °C. In total, six samples were annealed at four different temperatures: two at 248, two at 259 °C and two at 237 °C for 85 days then at 254 °C for 1.5 days. Since the samples that had the temperature changed did not have the recrystallisation fraction measured in between changing the temperatures, only after annealing at the last temperature, these two samples are given as the time–temperature combination 254 °C for 1.5 days in the model. These are the data points described as validation data points in Figure 3-16.

Table 3-5. Parameters in the model.

Parameter	Description	Initial guess (Excel)	Fitted value (Python)
t	time (days)		Durations from Table 3-2
X_s	recrystallised fraction		Fractions from Table 3-2
$t_{0.5}$	the time (days) taken to achieve a 0.5 recrystallised fraction		Calculated in Table 3-7
A	constant (fitting parameter) (days)	1.35982×10^{-57}	1.40483×10^{-54}
n	constant (fitting parameter)	1.579	1.445
Q	activation energy (fitting parameter) (J mol^{-1})	575 603.2	545 083.4
R	gas constant 8.314 (J mol^{-1} K^{-1})	n/a	n/a
T	Temperature (K)		Annealing temperatures from Table 3-2
$RMSE$	root mean square error	0.1501	0.1431
R^2	coefficient of determination	0.8332	0.8407

Table 3-6. Values of exponent n based on each temperature (from Excel calculations) with coefficients of determination, and the average used as initial guess.

Temperature (°C)	n	R^2
241	1.513	0.924
244	1.745	0.919
247	1.260	0.952
250	1.609	0.919
255	1.769	0.973
Average	1.579	

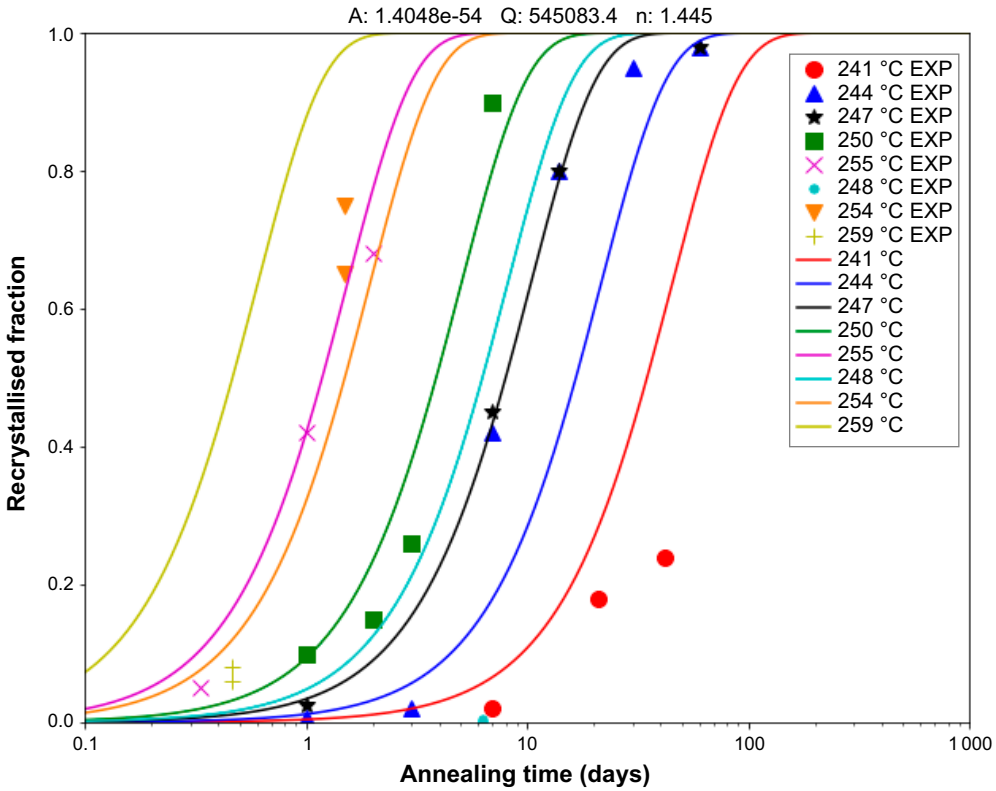

Figure 3-19. *Experimentally obtained recrystallised fractions (symbols) and fitted recrystallisation curves (lines) at different temperatures.*

Table 3-7. Prediction of duration to achieve 50 % recrystallised fractions according to Equation 2-2 using fitting parameters A and Q in Table 3-5, and the achieved recrystallisation (X_s) after annealing.

Temperature (°C)	$t_{0.5}$ (days)	X_s (%)	Comment
Annealing temperature	Predicted duration to achieve 50 % recrystallisation	Degree of recrystallisation observed after annealing	
237	94.96	Not available	Samples at 237 °C were stopped after 85 days and temperature increased to 254 °C for 1.5 days.
248	6.29	0.1, 0.5	
254	1.50	65, 75	
259	0.47	6, 8	

A comparison of predicted fractions and the experimentally observed fractions is shown in Figure 3-20. Time until 50 % recrystallisation according to the model (Equation 2-2) was calculated for a wider range of temperatures (Table 3-8). These durations were not validated by annealing additional samples in the present project, although comparison to results from Table 3-2 and Table 3-3 can be made. Recrystallised fractions after a time of 100 000 years, calculated by using Equation 2-1 and Equation 2-2 based on the fitted values (Python) of A, n and Q in Table 3-5, are shown in Table 3-9.

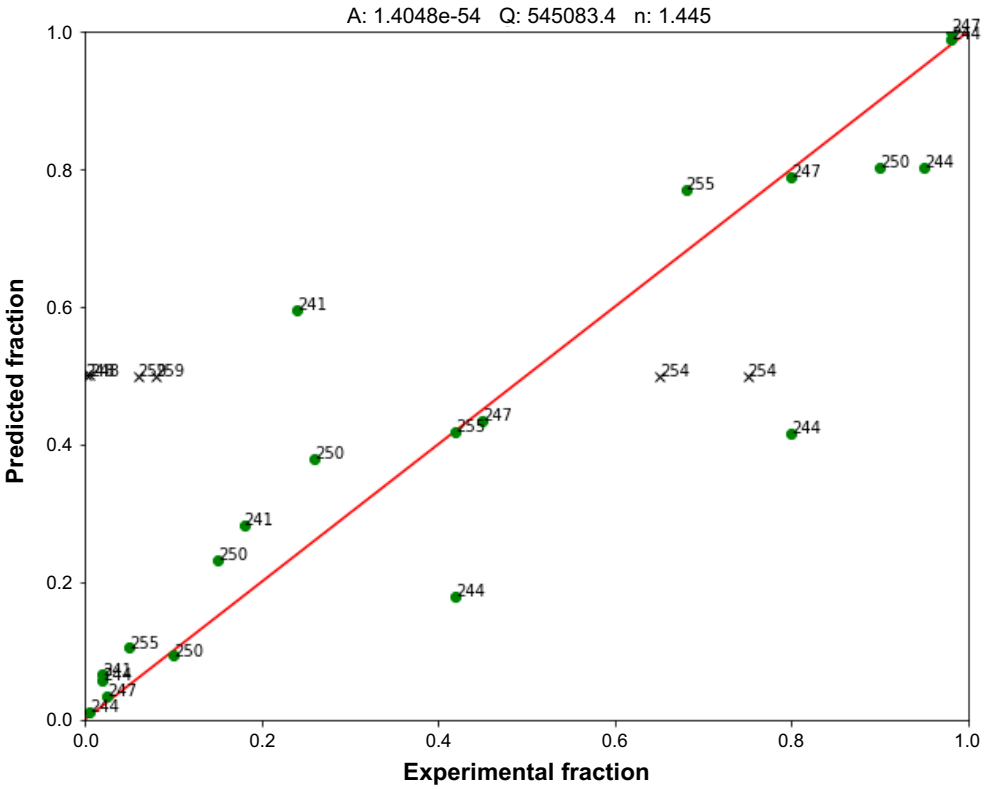

Figure 3-20. *Comparison of predicted and experimental values for the model fitted to the 20 data points in green circles. Validation data points, to which the model was not fitted, are plotted as black crosses. Numbers next to data points are temperatures in °C.*

Table 3-8. Time until 50 % recrystallised fraction ($t_{0.5}$) for several temperatures according to the model.

T (°C)	$t_{0.5}$ (days)
0	2.79×10^{50}
22	4.65×10^{42}
50	2.00×10^{34}
75	9.28×10^{27}
125	4.88×10^{17}
150	2.89×10^{13}
175	5.06×10^{9}
200	2.21×10^{6}
230	5.68×10^{2}
240	4.48×10^{1}
250	3.89×10^{0}
260	3.70×10^{-1}
350	7.10×10^{-9}
450	3.39×10^{-15}

Table 3-9. Fraction recrystallised (X_s) after 100 000 years for several temperatures according to the model.

T (°C)	X_s (%)
0	0
22	0
50	0
75	0
125	0
150	4.13×10^{-11}
175	1.11×10^{-5}
200	7.87×10^{-1}
230	100
240	100
250	100
260	100
350	100
450	100

4 Discussion

4.1 Recrystallisation and model

The discrepant results in this study warrant some discussion. First, results from 230 °C and 241 °C were found to be in contradiction to each other: for a given time, samples at 241 °C had no recrystallisation, while 230 °C at the same duration showed recrystallisation. After discussion with SKB, these data points from 230 and 241 °C were removed and a new batch of samples were annealed at 241 °C. The results from those samples were more consistent with the other results. Sources of error have been described in Chapter 2 but the cause for these discrepant results could not be determined.

In addition to this, the samples that were used for validation of the model also showed some strange results, at least for two of the temperatures (248, 259 °C). Only the samples that had been annealed for 85 days at 237 °C and then had the temperature increased to 254 °C, had results that were close to 50 %, as the model predicted. This could either point to the model having a low accuracy in this temperature range, which would be strange given that the annealing durations for the input data were in this temperature range. It could also be the case that something was wrong with the material or the furnaces' temperature control for these samples specifically. It could also be so that something was wrong for all or some of the samples used as input data to the model, which would give a lower accuracy of the model, although there is little indication that this was the case. The grain structure of the validation samples did not differ from other samples and the furnaces' temperature control were found to be good. The broken fans in the furnace, which could cause convection and temperature differences, should have been obviated by the way the temperature control was done, as described in Section 2.1.

It might be that the model is not so accurate at the beginning of the recrystallisation process when the development of recrystallisation is slow and when the rate of recrystallisation starts to change. At 255 °C, the degree of recrystallisation goes from 5 % after 1/3 day (8 hours) to 42 % after 1 day (24 hours). If the model's prediction is off by only a few hours, it could give a significantly different fraction after annealing at these temperatures. It might be easier to capture the behaviour for longer time durations or closer to 50 % recrystallisation where the rate is constant. The durations for the validating fractions were quite short (less than 1 week), but the predicted fractions were for 50 %, so evidently it could not predict the fractions well at 50 % for shorter durations.

Comparing the predicted and experimental fractions (Figure 3-20), the temperatures that have the worst fit, excluding the validation data points, are high fractions from 244 and 241°C, possibly indicating that for these temperatures, it was difficult to predict fractions between 0.2 (20 %) and 0.8 (80 %). Comparing 244 °C and 247 °C at similar fractions and durations, 247 °C is more accurate, and in general the fit is better for temperatures above 241 and 244 °C, i.e., for shorter durations. Given this, it is strange that the higher temperatures and short durations used for validation had such low fractions compared to the prediction of 50 %. It is also notable how similar 244 and 247 °C are to one another, while 241 °C had a much slower development of recrystallisation.

There are different values of the model's parameters that can be used, for example using only the initial guess from Excel without optimisation in Python or using values of n for every temperature rather than taking an average of all temperatures. While this work does not include a proper comparison of these variants, during the project it was not found to make a very large difference unless the initial guess gave curve fits that were not off by several orders of magnitude in time.

It might also be so that fitting to recrystallisation data requires a higher number of data points to give a good model. More samples were annealed at shorter durations: excluding the validating samples, 13 samples at less than or equal to 7 days, 7 samples at more than or equal to 14 days (Figure 3-16). The number of data points was also different for the temperatures, with 244 °C having six data points (highest fraction 0.98 at 60 days) while 241 °C had three data points (highest fraction 0.24 at 42 days). This lack of data from longer durations might make it difficult to predict at longer durations. The temperature range was also quite limited, from 241 to 255 °C (excluding validation data points), but this was chosen on purpose because recrystallisation at lower temperatures in Sundström et al. (2020) was found to be so slow that it was not viable to perform recrystallisation experiments at durations of

years in this project. Moreover, valuable data for longer durations from 230 °C were excluded because they were not deemed reliable, and only one sample from 195 °C was analysed (30 days, no recrystallisation); more samples from 195 °C could have been relevant to analyse.

Since a difference between two samples annealed at the same time in the same furnace was up to 10 percentage points (Table 3-7, 254 °C), such variation could shift the curves. Moreover, as described in Chapter 2, some recrystallised fractions (SEM images and EBSD data) were re-evaluated and the differences from a previous analysis were sometimes up to 5 and 10 percentage points, indicating the importance of having a single operator in the analyses. The size of area of analysis does not seem to have a large impact based on two samples where such a comparison was made, for 255 °C after 1 day annealing there was a difference of 1 percentage point (Figure 3-13, Figure 3-14) when a 10 times larger area was analysed, with the larger area having a lower fraction. For 254 °C after 1.5 days of annealing a difference of 6 percentage points was noted when a 32 times larger area was analysed, with the larger area having a lower fraction once again. However, this work does not include an analysis of how sensitive the model is to these variations.

Comparison to recrystallisation data from Table 3-3 with predictions for 50 % recrystallisation in Table 3-8 is possible. While the model could not accurately predict the duration for 50 % recrystallisation at 248 and 259 °C, or alternately something was wrong with the samples for these annealing temperatures, the model does predict 50 % recrystallisation nearly exactly at 350 and 450 °C. This can be compared with the results from Sundström et al. (2020), also in Table 3-3, where the samples were fully recrystallised after 1 day of annealing. Shorter time durations were not studied. A comparison to literature can be made here, where 99.90 % copper had recrystallised almost completely after a 93.75 % compression followed by annealing at 350 °C for 5 to 60 minutes (Li et al. 2023). Grain structures from the present study were quite similar to the 99.90 % copper after 93.75 % compression, but a more prominent layered banding was seen in Li et al. (2023), probably due to the larger reduction (Li et al. 2023). After annealing, grain sizes in the present study were larger (Figure 3-18), around 25 µm compared to 7 µm (Li et al. 2023). Hutchinson and Ray (1979) found a reduction in as-recrystallised grain size by the addition of phosphorus to pure copper, as phosphorus inhibits the growth of recrystallised grains. The larger grain size for Cu-OFP in the present work, compared to the smaller grain size seen in the pure copper in Li et al. (2023) is presumably explained by the annealing step at 600 °C prior to cold rolling in the present work, and possibly also the smaller reduction in the present work, 50 % compared to 93.75 % in Li et al. (2023). As in the present study, holding time was seen to have a very small effect on grain size (Li et al. 2023).

When comparing to the recrystallisation data that was used as input data, the fitting is good ($R^2 = 0.84$ in Table 3-5), which can also be visualised as a comparison of experimental and predicted fractions in Figure 3-20. At 250 °C, the model predicts 50 % recrystallisation after about 4 days which can be compared to the result of 26 % recrystallisation after 3 days. For 240 °C, a prediction of 45 days for 50 % recrystallisation was made, compared to a result of 24 % recrystallisation after 42 days at 241 °C. Recrystallisation proceeds rapidly once it has developed beyond the initial phase, so for these comparisons the model seems to be good, possibly underestimating the degree of recrystallisation somewhat. At the same time, the very low recrystallised fractions from 248 and 259 °C, and the previously discrepant results from 230 °C and 241 °C, together decreases the confidence in the model since a good explanation could not be found for these discrepant values.

It should be noted that deviation from the JMAK model is common because some assumptions it is based on are rarely valid, namely the spatially random distribution of nucleation sites (Humphreys et al. 2017). Instead, nucleation often occurs at prior grain boundaries, transition bands and shear bands and grain growth rates often decrease with time which leads to deviation from ideal JMAK behaviour (Humphreys et al. 2017). Furthermore, grains often recrystallise at different rates (Humphreys et al. 2017). There are alternatives to this model, but they will not be discussed here. It is not expected that the data conforms perfectly to the JMAK model.

Fine-grained materials tend to have a more homogenous recrystallisation than coarse-grained (Humphreys et al. 2017). Fine-grained oxygen-free high-conductivity (OFHC) copper with a grain size of 15 µm cold rolled to 93 % and annealed at 225 °C showed recrystallisation consistent with JMAK kinetics, but the coarse-grained variant (50 µm) showed deviation of slope n at both shorter and longer annealing times (Hutchinson et al. 1989), obtaining a value of $n = 1.72$ for the

coarse-grained material and n = 2.67 for the fine-grained. A value of 3 or higher for the exponent n is considered the ideal behaviour, but values of 2 or less are often found (Hutchinson et al. 1989) because of the reasons mentioned in the previous paragraph.

Grain size before annealing was not measured in the present work but large, elongated grains were observed (Figure 3-3) in lengths from 100 to 200 µm, which is expected given the high annealing temperature before rolling (600 °C). The grain size after annealing was around 25 µm. The value of the slope n (Table 3-6) varied from 1.26 to 1.76 in the present work depending on annealing temperature and was 1.51 at 241 °C, with R^2 values ranging from 0.92 to 0.97. It was difficult to say whether any deviation of slope – i.e., any explanation for lower values of R^2 for n in Table 3-6 – in the present work was related to longer or shorter annealing times as more samples would have been needed to make this judgment.

In Figure 3-5 recrystallised grains were seen to nucleate at grain boundaries, and it seems to have happened particularly at deformed areas which have black non-indexed pixels in the EBSD image. The locations of recrystallisation can also be seen in a larger sample shown in Figure 3-14, where a millimetre-sized area is shown from a sample that had been annealed for 24 hours at 255 °C, but it is difficult to say whether the locations are random or if there is some preference for certain sites. Some recrystallised grains are seen to be larger than others in Figure 3-9 and Figure 3-14, possibly indicating a difference in growth rates. Observations in high voltage electron microscopy have shown that phosphorus-alloyed copper had recrystallisation growth rates that were not constant, but instead had high growth rates after nucleation which slowed down rapidly, even when the recrystallised grains were surrounded by deformed substructure (Hutchinson and Ray 1979). Grains in pure copper grew with a steady rate until the recrystallised grain impinged on other recrystallised grains.

A study on 99.90 % copper that had undergone 93.75 % compression followed by annealing at 350 °C showed that the distribution of dislocation density inside grains was correlated with recrystallisation (Li et al. 2023). The compressed copper had preferred orientations, with some grains preferentially deforming (Li et al. 2023). This could possibly give a recrystallisation behaviour that is not homogenous since different texture components can recrystallise at different rates and the spatial distribution of orientations can affect both initiation and growth of recrystallised grains (Humphreys et al. 2017). While the assumptions of the JMAK model are rarely fulfilled, it probably does not explain the clearly discrepant fractions from 248 and 259 °C, and the previously discrepant results from 230 °C and 241 °C.

The activation energy found for Cu-OFP according to the curve fits in this work, 545 kJ mol^{-1}, is very high compared to values found in literature. A value of 129 kJ mol^{-1} was found for 99.999 % copper after 39.5 % elongation and annealing at 170 or 180 °C, giving recrystallised fractions of 30 to 60 % (Gordon 1955). The same study found the recrystallisation energy to be independent of strain in the range of 17.5 to 39.5 % elongation, and that the recrystallised fraction did not affect the activation energy (Gordon 1955). Samples with lower elongation had a slower recrystallisation, for example to obtain 60 % recrystallisation a 10-hour annealing duration at 180 °C was required after 30 % elongation, but after 39.5 % elongation only 2 hours were required.

Differences between the current work and the comparison are the material used (Cu-OFP compared to 99.999 % copper), amount and type of strain (up to 40 % tensile elongation compared to 50 % compressive reduction), annealing temperatures, durations and possibly also the initial grain size before annealing. Impurities can increase the activation energy in copper (Gordon 1955) and it is often observed that solutes reduce grain boundary mobility (Humphreys et al. 2017), which retards recrystallisation. The softening temperature is known to increase due to addition of phosphorus (Smart and Smith 1946, MNC 1987). For copper doped with much higher amounts of phosphorus, 1 600 and 7 600 ppm, than the Cu-OFP used in the present study with 50 ppm phosphorus, cold rolled to a reduction of 95 % and annealed to temperatures ranging from 175 to 325 °C, it was found that the activation energy was 151 kJ mol^{-1}, which was almost double that of the 99.998 % pure copper in the same study, at 80 kJ mol^{-1} (Hutchinson and Ray 1979).

The model was used to estimate time until recrystallisation at a range of temperatures. The model predicts that at 175 °C, the duration until 50 % recrystallisation is on the order of 10^6 years. After 100 000 years at 175 °C, the recrystallised fraction would be 10^{-5} %. The lack of recrystallisation found in samples at temperatures from 75 to 175 °C for durations up to 6 months (Sundström et al. 2020)

supports this. Even at 200 °C, the model predicts less than 1 % recrystallisation after 100 000 years. While the accuracy of these predictions may not be high, or is unknown, with regards to the precise number of years and amount of recrystallisation, the general impression is that for temperatures of 175 °C and below, recrystallisation does not seem likely to occur even at very long-time scales in Cu-OFP.

4.2 Hardness

The recrystallisation development correlated well with the hardness measurements. The change in microstructure at 244 and 247 °C after one day is reflected in the hardness which decreases. The hardness measurements agreed well with the metallographic investigation. At 244 and 247 °C the hardness decreases after the first duration of 1 day, which corresponds to the recrystallisation that starts at 1 day for both 244 and 247 °C. It is also possible that recovery has some role in the softening. Recovery is a process that involves annihilation of dislocations (Humphreys et al. 2017). It is a process that competes with recrystallisation, and there can be no recovery once recrystallisation has been completed (Humphreys et al. 2017). Copper has a low stacking fault energy, which results in little recovery before recrystallisation. Solutes such as phosphorus can alter this behaviour, but the net effects on recovery are mixed and will depend on material and solute atom (Humphreys et al. 2017). Recovery in copper can cause a slight increase in hardness or no change at all (Davis 2001). Recovery was found to have had no impact on hardness in 99.999 % copper (Gordon 1955), but recovery also had a limited role in this material as indicated by stored energy measurements during annealing (Gordon 1955). The same study concluded that the ratio between the stored energy of recovery and recrystallisation was larger in copper of lower purity, i.e., recovery was more prominent in coppers with lower purity (Gordon 1955). This means that Cu-OFP, being less pure, could exhibit recovery of hardness because of the presence of phosphorus. For copper with 1 600 and 7 600 ppm phosphorus compared to a 99.998 % pure copper, cold rolled to 95 % reduction and annealed at 250 °C, time until 50 % recrystallisation and 50 % recovery was four orders of magnitude greater for the phosphorus-alloyed coppers than the pure copper (Hutchinson and Ray 1979). In summary, recovery might have a greater role in phosphorus-doped copper than in pure copper, but it remains unclear whether it had any effect on hardness in the present work.

There is large variation in the hardness measurements. This could reflect issues during measurements, e.g., keeping the surface planar to the indenter, but could also be because of the microstructure and the low weight used, e.g., sampling grains with different orientations or sampling both recrystallised and non-recrystallised grains. This variation was extensively studied and discussed in the previous study (Sundström et al. 2020), including statistical analysis. Some more detailed argumentation on the causes of this variation is made here. According to the standard for Vickers hardness measurements (ISO 2018), the accuracy in determining the mean diagonal length is unlikely to be better than ± 1 µm. According to the standard a difference in diagonal length of more than 5 % should be explicitly stated in the test report and 1 µm of a 40 µm diagonal, a typical diagonal length for the recrystallised specimens, would account for a 2.5 % error alone. In terms of hardness values this would be errors on the order of a few HV, not more than 10 HV, in these measurements. This clearly does not explain all variation even if it accounts for some of it. The variation or range in hardness measurement is lowest for the shortest and longest durations, so it is reasonably explained by something that happens in between: recrystallisation. The non-recrystallised copper has a high degree of texture (anisotropy) caused by deformation during rolling. The size of a 0.05 HV indentation in annealed copper is ca 29 × 29 µm (Sundström et al. 2020) and it has a square shape. The distance between each indentation was 800 µm, so there are on average more than 25 grains between each measurement. The mean grain size of copper annealed at temperatures of around 240 to 250 °C is around 25 µm, while the smallest grains are a few microns and the largest are hundreds of microns. The size of the indentation decreases with material hardness. This means that the size of the indentation may have been small enough that a single measurement is a measurement from a single grain. In that case, if 5 measurements are made on one specimen that has partially recrystallised, a freshly recrystallised and a non-recrystallised deformed structure may be sampled in different measurements, explaining the range in hardness observed.

The uncertainty in sectioning, i.e., whether it was the rolling direction or transverse direction that was measured, could also contribute to the spread in hardness values. The scatter is lowest for the samples (1) annealed at 600 °C, (2) annealed at 600 °C and then cold rolled and (3) for the samples annealed at lower temperatures for the shortest and longest durations, corresponding to little and near complete recrystallisation respectively for both 244 °C and 247 °C. The samples annealed at 600 °C and annealed at 600 °C then cold rolled have a similar grain structure, completely recrystallised in the former case, and fully deformed in the latter. The low scatter seen in these samples and the high scatter seen in the other samples seems to support the notion that a mix of deformed substructure and freshly recrystallised grains can give increased scatter in micro-hardness measurements.

Some comparison to a study on 99.999 % copper can be made (Gordon 1955), where micro-hardness was used to assess the recrystallised fraction after 10.8 % elongation and annealing at 210 °C. Hardness for unrecrystallised as deformed samples were approximately normally distributed about a mean of 70 Vickers hardness, and completely recrystallised samples had a mean hardness of 45 with a broader normal distribution than that of the unrecrystallised as deformed. The distributions did not overlap each other. As recrystallisation proceeded, hardness values in between these two groups were measured, showing a clear relationship between recrystallisation development and hardness. At 56.6 % recrystallised fraction, hardness values from both distributions and values in between were measured, with a range from about 40 to 90 Vickers hardness. This indicates that in samples with a mix of unrecrystallised and recrystallised grains, a large scatter in hardness values can be found. Another study (Li et al. 2023) performed hardness measurements on 99.90 % copper after large compressive deformations of 93.75 % and annealing at 350 °C for durations ranging from 5 to 60 minutes. They found hardness values similar to the present study, though with lower scatter.

5 Conclusions

Samples from two temperature–time combinations that were used to validate the model had much lower degree of recrystallisation than expected and this has not been explained, so ultimately the model could not be validated. Nonetheless, the model and recrystallisation results from lower temperatures (75 to 175 °C) still show that recrystallisation does not seem likely for Cu-OFP at the temperatures that occur in the repository even for very long-time scales.

References

SKB's (Svensk Kärnbränslehantering AB) publications can be found at www.skb.com/publications.

Bowyer W H, 1999. The effects of impurities on the properties of OFP copper specified for the copper iron canister. SKI Report 99:44, Statens kärnkraftinspektion (Swedish Nuclear Power Inspectorate).

Davis J R (red), 2001. Copper and copper alloys. Materials Park, OH: ASM International.

Gordon P, 1955. Microcalorimetric Investigation of Recrystallisation of Copper. Trans. Metall. Soc. AIME 203, 1043.

Hagström J, Sandström R, Sarnet J, 2022. Microstructure and crystallographic variations in different positions in OFP copper outer shell of canisters for spent nuclear fuel storage. Copper Alloys Conference 2022.

Honeycombe R W K, 1968. The plastic deformation of metals, 1st ed, Edward Arnold Publishers, Ltd.

Humphreys F John, Gregory S Rohrer, Anthony D Rollett, 2017. Recrystallisation and Related Annealing Phenomena. 3. ed. Amsterdam: Elsevier.

Hutchinson W B, Ray R K, 1979. Influence of phosphorus additions on annealing behaviour of cold-worked copper. Metal Science, 13(3–4), 125–130. https://doi.org/10.1179/msc.1979.13.3-4.125

Hutchinson W B, Jonsson S, Ryde L, 1989. On the kinetics of recrystallisation in cold worked metals. Scr. Metall. 23, 671.

ISO 6507-1:2018. Metallic materials – Vickers hardness test – Part 1: Test method.

Jonsson M, Emilsson G, Emilsson L, 2018. Mechanical design analysis for the canister. Posiva SKB Report 04, Posiva Oy, Svensk Kärnbränslehantering AB.

Levenberg K, 1994. A Method for the Solution of Certain Non-Linear Problems in Least Squares. Quarterly of Applied Mathematics, vol. 2, no. 2, 1944, pp. 164–68. JSTOR, http://www.jstor.org/stable/43633451

Li X, Zhang Q, Lou W, Li F, Liang J, Gu S, 2023. Microstructure and Texture of Pure Copper under Large Compression Deformation and Different Annealing Times. Coatings 13:2093. https://doi.org/10.3390/coatings13122093

MNC, 1987. Koppar och kopparlegeringar: Copper and copper alloys. 2. utg. Stockholm: Metallnormcentralen och Standardiseringskommissionen i Sverige (SIS).

Rowe G W, 1977. Principles of industrial metalworking processes. London: Edward Arnold.

SKB, 2006. Long-term safety for KBS-3 repositories at Forsmark and Laxemar – a first evaluation. Main report of the SR-Can project. SKB TR-06-09, Svensk Kärnbränslehantering AB.

Smart J S, Smith A A, 1946. Effect of phosphorus, arsenic, sulphur, and selenium on some properties of high-purity copper. Transactions of the American Institute of Mining, Metallurgical and Petroleum Engineers 166, 144–155.

Sundström R, Andersson-Östling H C M, Hagström J, 2020. Recrystallisation of copper with phosphorus and Auger microscopy studies of the phosphorus content. SKB TR-20-07, Svensk Kärnbränslehantering AB.

Arkitektkopia AB, Bromma, 2024

SKB is responsible for managing spent nuclear fuel and radioactive waste produced by the Swedish nuclear power plants such that man and the environment are protected in the near and distant future.

skb.se